

Scalar fields in a non-commutative space

Wolfgang Bietenholz^a, Frank Hofheinz^b,
Héctor Mejía-Díaz^a and Marco Panero^c

^a Instituto de Ciencias Nucleares, Universidad Nacional Autónoma de México
A.P. 70-543, C.P. 04510 México, Distrito Federal, Mexico

^b Institute of Radiopharmaceutical Cancer Research
Helmholtz-Zentrum Dresden-Rossendorf, Germany

^c Instituto de Física Teórica UAM/CSIC, Universidad Autónoma de Madrid
Ciudad Universitaria de Cantoblanco, 28049 Madrid, Spain

E-mail: wolbi@nucleares.unam.mx

Abstract. We discuss the $\lambda\phi^4$ model in 2- and 3-dimensional non-commutative spaces. The mapping onto a Hermitian matrix model enables its non-perturbative investigation by Monte Carlo simulations. The numerical results reveal a phase where stripe patterns dominate. In $d = 3$ we show that in this phase the dispersion relation is deformed in the IR regime, in agreement with the property of UV/IR mixing. This “striped phase” also occurs in $d = 2$. For both dimensions we provide evidence that it persists in the simultaneous limit to the continuum and to infinite volume (“Double Scaling Limit”). This implies the spontaneous breaking of translation symmetry.

1. Quantum physics in a non-commutative space

Since in standard quantum mechanics the operators of space and momentum coordinates do not commute, it seems like an obvious idea to “quantise further” by also introducing non-zero commutators among space coordinates (or among momentum coordinates) in different directions. Hence it is not surprising that this idea dates back to the 1940s. Its pre-history involves famous names like Heisenberg, Pauli, Peierls and Oppenheimer, and in 1947 the first papers on this subject were published [1].

However, the consequences of non-commutative (NC) geometry in quantum field theory are extremely involved. Here we consider only the simplest case of two NC spatial coordinates, with a constant non-commutativity “tensor” Θ ,

$$[\hat{x}_i, \hat{x}_j] = i\Theta_{ij} = i\theta\epsilon_{ij}, \quad (1.1)$$

where \hat{x}_i are Hermitian operators, $i, j \in \{1, 2\}$, and θ is the non-commutativity parameter.

In the 1980s deep mathematical work was carried out about the formal formulation of field theories on such spaces (for a review, see Ref. [2]). Applications were discussed in solid state physics, in particular related to the quantum Hall effect, see *e.g.* Ref. [3]. Of course, in this context one actually deals with the usual geometry, but a magnetic background field B can be interpreted as $\theta \propto 1/B$, which leads to NC canonical coordinates.

In the period from 1996 to 1998 a boom of interest in NC field theories set in, which led to about 3000 papers on this subject up to now [4]. This boom was triggered by the observation



that low energy string theory can be related to NC field theory [5], following the spirit of the re-interpretation of the magnetic background field.

Here we are going to address NC field theory as such; no strings attached. A qualitative difference from usual field theory is its *non-locality*; fields interact at distinct points over a characteristic distance $\sim \sqrt{\|\Theta\|}$. This entails frightening conceptual problems. On the other hand, from a very optimistic point of view, this is just what it takes for a proposal to formulate quantum gravity.

In this regard, we mention a simple *Gedankenexperiment*: assume some event to be measured with extremely tiny space-time uncertainties $\Delta x_1, \Delta x_2, \Delta x_3, \Delta t$, on the order of the Planck length $l_{\text{Planck}} \simeq 1.6 \cdot 10^{-35}$ m. This requires a huge energy density, so gravitation should be taken into consideration. In the extreme case this could yield an event horizon, which is larger than the Heisenberg uncertainties, so the event is invisible. According to Ref. [6], avoiding that scenario requires

$$\begin{aligned} \Delta x_1 \Delta x_2 + \Delta x_1 \Delta x_3 + \Delta x_2 \Delta x_3 &\geq l_{\text{Planck}}^2, \\ (\Delta x_1 + \Delta x_2 + \Delta x_3) \Delta t &\geq l_{\text{Planck}}^2. \end{aligned} \quad (1.2)$$

Such space-time uncertainties are characteristic for an NC space. Is this a natural framework for the conciliation of quantum theory and gravity? We should add, however, that much of the literature on this subject keeps the time commutative. That deviates from the above consideration, but it may save unitarity and reflection positivity, and it alleviates the problems related to causality.

The historic motivation, however, was different. People hoped that washing out the space-time points in this way¹ could remove (or at least weaken) the notorious UV divergences in quantum field theory, and avoid (or simplify) renormalisation. This turned out to be wrong: renormalisation is not getting easier, but much harder due to non-commutativity. First of all, in planar diagrams of a perturbative expansion, the UV divergences simply persist [7]. Second, in the non-planar diagrams they tend to “mix” with IR divergences. This type of singularities does not occur in the commutative world, and it is very difficult to deal with. For a simple intuitive picture, we start again from the Heisenberg uncertainty $\Delta x_i \sim 1/\Delta p_i$, and we combine it with

$$\Delta x_i \sim \Theta_{ij} / \Delta x_j \sim \Theta_{ij} \Delta p_j \quad (i \neq j). \quad (1.3)$$

Therefore an attempt to squeeze $\Delta p_i \rightarrow 0$ makes Δp_j diverge. Due to such mixed singularities, the renormalisation of multi-loop diagrams is mysterious. Hence it is highly motivated to adopt a fully *non-perturbative approach*.

In many models, the lattice regularisation enables the non-perturbative treatment of quantum field theory. So let us introduce a lattice structure also on the NC plane of eq. (1.1) (this concept is reviewed in Ref. [8]). This is achieved — at least in a fuzzy form — if we impose the operator identity

$$\exp\left(i \frac{2\pi}{a} \hat{x}_i\right) = \hat{1}. \quad (1.4)$$

For lattice spacing a we expect periodicity of the (commutative) momentum components over the Brillouin zone,

$$\exp\left(i \sum_i k_i \hat{x}_i\right) = \exp\left(i \sum_i \left(k_i + \frac{2\pi}{a}\right) \hat{x}_i\right), \quad i = 1, 2. \quad (1.5)$$

¹ Some people denote it as “pointless geometry”.

Multiplication with the inverse factor $\exp(-i\sum_j k_j \hat{x}_j)$ from the right, and applying the Baker-Campbell-Hausdorff formula, leads to

$$\hat{\mathbb{1}} = \hat{\mathbb{1}} \exp\left(\frac{i\pi}{a}\theta(k_2 - k_1)\right) \Rightarrow \frac{\theta}{2a}k_i \in \mathbb{Z}. \quad (1.6)$$

Therefore, in contrast to the commutative space, the NC lattice is automatically *periodic*.

If we now assume periodicity over the lattice volume $N \times N$, we have discrete momenta $k^{(n)} = \frac{2\pi}{aN}n$, $n \in \mathbb{Z}^2$, and we arrive at the relation

$$\theta = \frac{1}{\pi}Na^2. \quad (1.7)$$

In order to keep θ finite, in particular for $\theta = \text{const.}$, we have to take the limits to the continuum, $a \rightarrow 0$, and to infinite volume, $Na \rightarrow \infty$, *simultaneously*. This is the *Double Scaling Limit*,

$$\left. \begin{array}{l} a \rightarrow 0 \\ N \rightarrow \infty \end{array} \right\} \text{ such that } Na^2 = \text{const.}, \quad (1.8)$$

which leads to a NC plane of infinite extent. Clearly, this requirement is again related to the property of UV/IR mixing. Taking these limits differently, one would usually end up with $\theta = 0$ or $\theta = \infty$, which are both (different) cases of commutative field theory. For a consistent study of NC field theory, we have to follow the instruction (1.8).

2. The non-commutative $\lambda\phi^4$ model

2.1. Formulation

NC field theory can be formulated such that the fields are functions of the standard (commutative) coordinates x_μ , if all field multiplications are performed by *star products* (or *Moyal products*). A prototype reads

$$\phi(x) \star \psi(x) := \phi(x) \exp\left(\frac{i}{2} \overleftarrow{\partial}_\mu \Theta_{\mu\nu} \overrightarrow{\partial}_\nu\right) \psi(x) \quad (2.1)$$

(for instance $[x_\mu, x_\nu]_\star = i\Theta_{\mu\nu}$). This can be justified with a plane wave decomposition.

For bilinear terms under a space-time integral (without boundary terms) the star product is equivalent to a simple product, because of the anti-symmetry of Θ . Hence the action of the $\lambda\phi^4$ model in NC Euclidean space can be written as

$$S[\phi] = \int d^d x \left[\frac{1}{2} \partial_\mu \phi \partial_\mu \phi + \frac{m^2}{2} \phi^2 + \frac{\lambda}{4} \phi \star \phi \star \phi \star \phi \right]. \quad (2.2)$$

This shows that the parameter λ does not only determine the strength of the self-interaction, but also the extent of NC effects.

The perturbative expansion of this model has been discussed extensively in the literature. Regarding the 1-loop diagrams, there is a planar contribution, which takes the standard form [7], as we mentioned before. On the other hand, the non-planar diagrams pick up a phase factor due to the non-commutativity. For the moment, let us introduce a momentum cutoff Λ . Then the 1-loop integrals and their leading divergences in $d = 4$ take the form [9]

$$\text{planar : } \int d^d k \frac{1}{k^2 + m^2} \propto \Lambda^2, \quad \text{non-planar : } \int d^d k \frac{\exp(ik_\mu \Theta_{\mu\nu} p_\nu)}{k^2 + m^2} \propto \frac{1}{1/\Lambda^2 + p_\mu \Theta_{\mu\nu} p_\nu}.$$

We see that a finite Θ does indeed allow us to take the limit $\Lambda \rightarrow \infty$ in the non-planar part. However, then a singularity emerges for external momentum $p \rightarrow 0$, which illustrates the UV/IR

mixing. Moreover, even at finite p , the limit $\Theta \rightarrow 0$ is not smooth; therefore the meaning of a truncated expansion in small $\|\Theta\|$ is questionable. Finally we also confirm that the opposite limit $\Theta \rightarrow \infty$ is commutative, but different from $\Theta = 0$.

Now we consider $d = 3$, so that the scalar field $\phi(\vec{x}, t)$ lives on a NC plane (x_1, x_2) , plus a commutative Euclidean time t . We assume a lattice structure, for the NC plane as described in Section 1, and for the time in a regular form. The action on a $N^2 \times T$ lattice can be mapped (with identical algebras) onto a matrix model with twisted boundary conditions [10],

$$S[\bar{\phi}] = \text{Tr} \sum_{t=1}^T \left[\frac{1}{2} \sum_{i=1}^2 \left(\Gamma_i \bar{\phi}(t) \Gamma_i^\dagger - \bar{\phi}(t) \right)^2 + \frac{1}{2} \left(\bar{\phi}(t+1) - \bar{\phi}(t) \right)^2 + \frac{m^2}{2} \bar{\phi}^2(t) + \frac{\lambda}{4} \bar{\phi}^4(t) \right], \quad (2.3)$$

where $\bar{\phi}(t)$ are Hermitian $N \times N$ matrices, located at $t = 1, \dots, T$ (we are using lattice units). The kinetic term has the standard lattice form in time direction, but in the NC plane it is constructed by means of so-called twist eaters Γ_i . They arrange for a shift by one lattice unit, if they obey the 't Hooft-Weyl algebra

$$\Gamma_i \Gamma_j = Z_{ji} \Gamma_j \Gamma_i. \quad (2.4)$$

Here the twisted boundary conditions enter, and we choose the corresponding phase factor as

$$Z_{21} = Z_{12}^* = \exp \left(i\pi(N+1)/N \right), \quad (2.5)$$

where the size N is assumed to be odd. Then we insert a unitary solution for Γ_1 and Γ_2 , which is known as clock- and shift-matrix (they are written down explicitly *e.g.* in Refs. [10, 11]). The crucial property, however, is relation (2.4).

2.2. Phase diagram

Some years ago, Gubser and Sondhi performed a 1-loop calculation in the Hartree-Fock approximation [12] and conjectured the following properties of the phase diagram of the NC $\lambda\phi^4$ model in $d = 3$ and 4:

- At small θ , there is an Ising-type phase transition between a disordered and a uniform phase at some critical value $m_c^2 < 0$ (a strongly negative parameter m^2 can be interpreted as low temperature).
- At large θ and some $m_c^2 < 0$, there is another phase transition, but now between a disordered and a *striped phase*.

Further considerations were added with Renormalisation Group techniques [13], and with the Cornwall-Jackiw-Tomboulis effective action approach [14]. They are consistent with the qualitative picture by Gubser and Sondhi.

A *quantitative* study was based on Monte Carlo simulations, which probed the phase diagram in the (m^2, λ) plane, for the 3d matrix formulation described in Subsection 2.1, at $N = T = 15 \dots 45$ [11]. Thus the picture by Gubser and Sondhi is converted into a uniform/disordered transition at small λ , and a striped/disordered transition at large λ . This is in fact observed, as the phase diagram in Figure 1 shows. Figure 2 adds the features of typical configurations in the four sectors (after mapping back the matrices to a lattice scalar field).

The phases, and their transitions, were identified with the momentum dependent order parameter

$$M(k) = \frac{1}{NT} \max_{\frac{N}{2\pi}|\vec{p}|=k} \left| \sum_t \tilde{\phi}(\vec{p}, t) \right|. \quad (2.6)$$

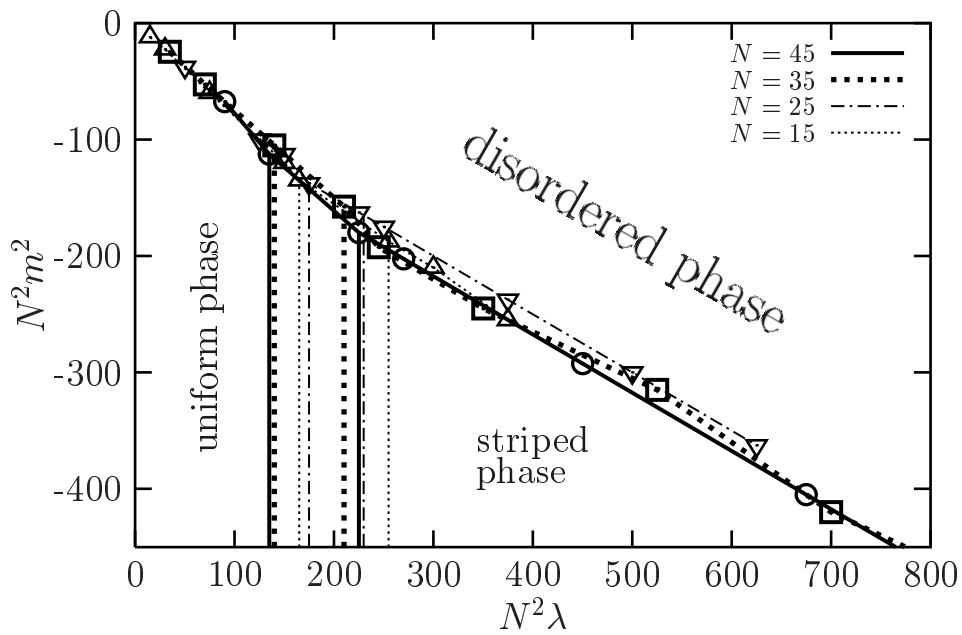


Figure 1. The phase diagram of the 3d $\lambda\phi^4$ model on an NC plane but with a commutative Euclidean time coordinate. The ordered regime — at strongly negative $N^2 m^2$ — is divided into phases of uniform and of striped order.

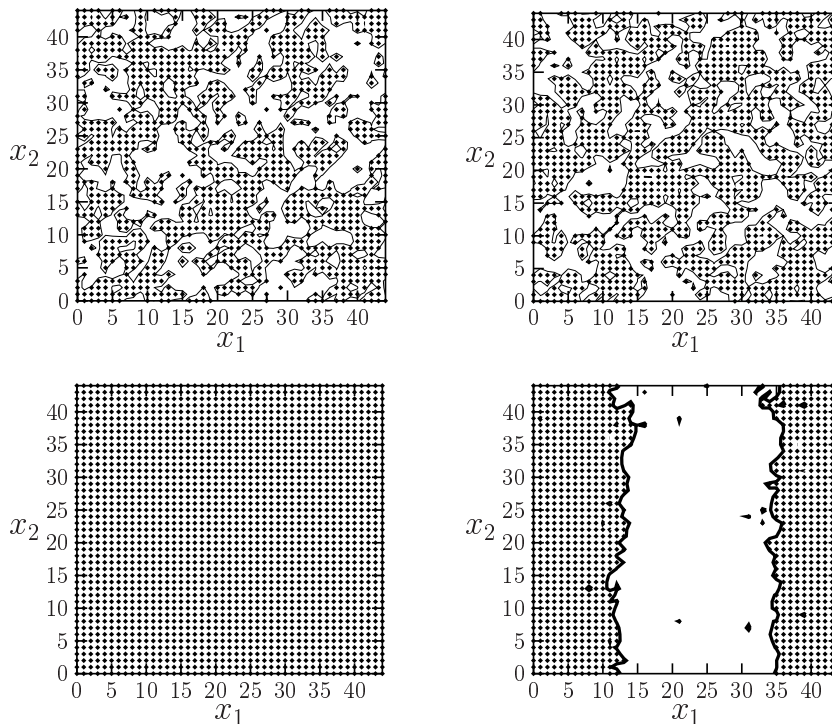


Figure 2. Typical configuration of the 3d $\lambda\phi^4$ model at $N = T = 45$: we show the NC plane, and dark/bright areas correspond to the two signs of ϕ . The examples on the left (right) refer to low (high) λ , and the upper (lower) plots were obtained at weakly (strongly) negative m^2 .

For $k = 0$ this is the magnetisation, and for finite k it captures the possible dominance of a “stripe pattern”, *e.g.* with k parallel stripes, rotated in a suitable way (if two non-zero components of \vec{p} are involved, the pattern is actually of a checker-board type).

Far from the transition lines, $M(k)$ indicates the phase unambiguously. The transition is identified best by varying $m^2 < 0$ at fixed λ , and searching for a peak in the connected two-point function

$$\langle M(k)^2 \rangle_{\text{con}} = \langle M(k)^2 \rangle - \langle M(k) \rangle^2 . \quad (2.7)$$

This provides accurate results for the critical values m_c^2 . For all λ values that we considered, this transition appears to be of second order.

On the other hand, the transition uniform/striped inside the ordered regime is rather hard to explore, as the uncertainty band in Figure 1 shows. Here we studied the thermal cycle, which reveals a clear hysteresis effect [11]; this is characteristic for a first order transition.

Next we considered the correlation functions close to the order/disorder transition, in the disordered regime (where finite size effects are harmless). Figure 3 refers to the spatial separation, and shows that the correlator

$$C(x_1, 0) = \langle \phi(\vec{0}; t) \phi(x_1, 0; t) \rangle \quad (2.8)$$

has an unusual shape, both close to the uniform and close to the striped phase. The decay is fast, but not exponential; it is NC distorted.

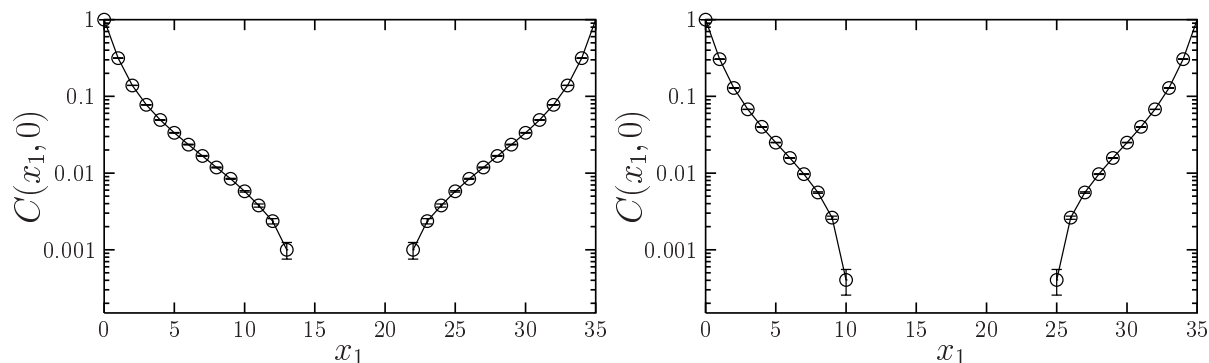


Figure 3. The correlation function $C(x_1, 0)$ for spatial separation, given in eq. (2.8). Both plots were obtained in the disordered phase, close to the ordering transition, at $N = T = 35$. On the left the parameters are $N^2 \lambda = 70$, $N^2 m^2 = -17.5$ (close to the uniform phase), and on the right $N^2 \lambda = 3500$, $N^2 m^2 = -140$ (close to the striped phase). In both cases, the decay is fast, but not exponential.

Nevertheless we can evaluate the energy based on the *temporal* correlation function. Here we first transform the spatial part of the configurations to momentum space, and we consider

$$G(\tau) = \langle \tilde{\phi}(\vec{p}, t) \tilde{\phi}(\vec{p}, t + \tau) \rangle . \quad (2.9)$$

Now we do find an exponential decay — respectively a cosh function behaviour at finite T — as Figure 4 illustrates for the example $\vec{p} = \vec{0}$.

This leads to the dispersion relation $E^2(\vec{p}^2)$ shown in Figure 5, now for $N = T = 55$. In fact, the energy minimum is located at *non-zero* \vec{p} , which is a clear indication that we are close to the striped phase; decreasing m^2 then leads to the condensation of a corresponding striped pattern.

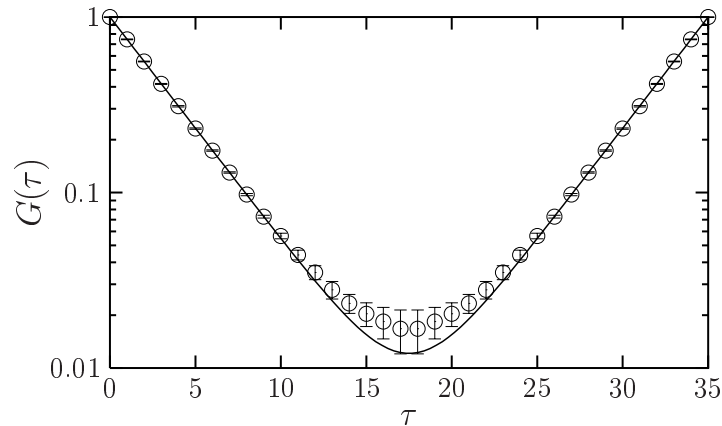


Figure 4. The temporal correlation function $G(\tau)$, given in eq. (2.9), measured at $N = T = 35$, $N^2\lambda = 350$, $N^2m^2 = -140$. The data agree very well with a cosh-fit.

It is evident that this pattern is non-uniform, but for the exact structure of the stripes various options are in close competition.

At very small momenta, the dispersion relation is consistent with the expected IR divergence.

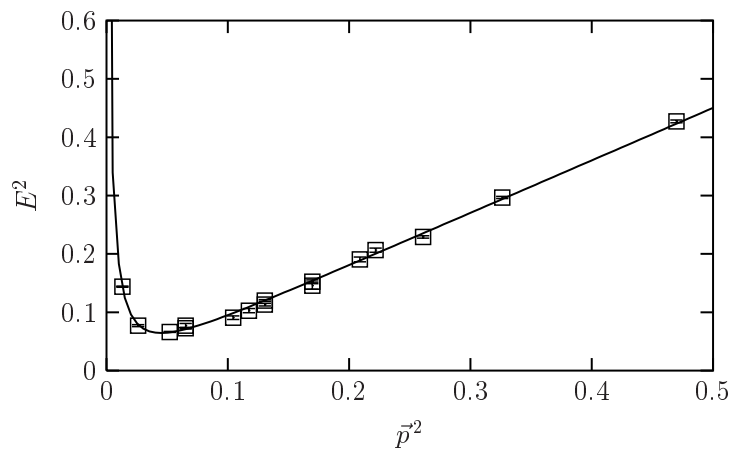


Figure 5. The dispersion relation $E^2(\vec{p}^2)$ determined at $N = T = 55$, $m^2 = -15$, $\lambda = 50$ (close to the striped phase). The energy takes its minimum at finite momentum, which leads to a striped pattern at somewhat lower m^2 . A 4-parameter fit [11] is consistent with the trend to an IR divergence in infinite volume.

2.3. Double Scaling Limit

So far we have been dealing with lattice units. In order to take a continuum limit, we have to introduce a scale, *i.e.* we need a dimensional reference quantity. For this reason, we extrapolate the (broad) linear regime in the dispersion relation $E(|\vec{p}|)$ down to $\vec{p} = \vec{0}$. This linear extrapolation deviates from the dispersion at small momenta, but it defines an effective mass M_{eff} , according to

$$E^2 = M_{\text{eff}}^2 + \vec{p}^2. \quad (2.10)$$

We are going to investigate the behaviour if m^2 approaches m_c^2 from above. Hence it is convenient to define

$$\Delta m^2 := m^2 - m_c^2 . \quad (2.11)$$

At fixed λ , and for $\Delta m^2 \gtrsim 0$, we observed the proportionality relation

$$M_{\text{eff}}^2|_{\lambda=\text{const.}} \propto \Delta m^2 , \quad (2.12)$$

as Figure 6 shows for $\lambda = 50$, as an example.

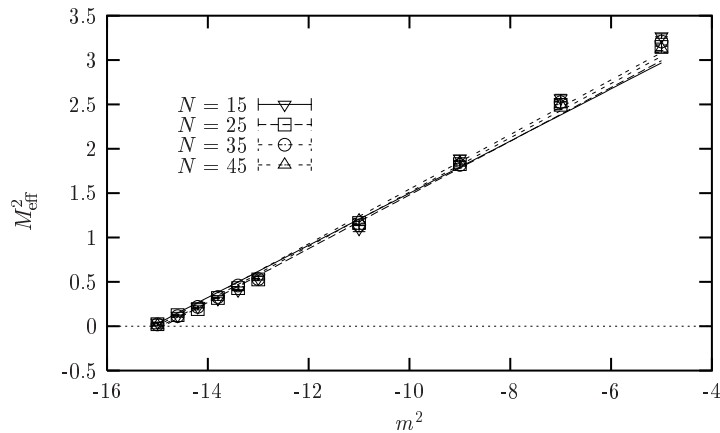


Figure 6. The effective mass squared, M_{eff}^2 , obtained by the extrapolation (2.10) of the dispersion relation. We see that M_{eff}^2 depends linearly on m^2 resp. on Δm^2 . The plot refers to $\lambda = 50$, where M_{eff}^2 vanishes at $m_c^2 = -15.01(8)$.

Now we can take a continuum limit by keeping the effective mass in dimensional units, M_{eff}/a , fixed. For simplicity we set this ratio to 1, hence $a = M_{\text{eff}}^{-1}$ is the dimensional lattice spacing. Therefore, the DSL condition $\theta \propto Na^2 = \text{const.}$ is implemented by increasing N , and simultaneously decreasing m^2 so that it approaches m_c^2 from above, in such a manner that

$$N \Delta m^2 = \text{const.} . \quad (2.13)$$

Now we can re-consider the dispersion relation in dimensional units. The rest energy diverges like $E(|\vec{p}| \rightarrow 0)/a \propto \sqrt{N}$ [11], which confirms the UV/IR mixing also dimensionally. For a broad range of finite momenta $|\vec{p}|/a$, Figure 7 shows that the dispersion relation stabilises if we approach the DSL, and that the energy minimum is obtained around the dimensional momentum

$$\vec{p}^2/a^2 \lesssim 0.1 M_{\text{eff}}^2 . \quad (2.14)$$

This tells us that the striped phase persists in the DSL, where stripes of finite width dominate. This observation implies the spontaneous breaking of translation and rotation symmetry in the striped phase of the 3d phase diagram.

That phenomenon leads to a tricky question: does the same happen also in $d = 2$? The next section will be devoted to this issue.

3. Does translation symmetry break in $d = 2$?

The Mermin-Wagner Theorem [15] tells us that usually a continuous global symmetry cannot break spontaneously in $d = 2$. At first sight this seems to imply that the striped phase cannot

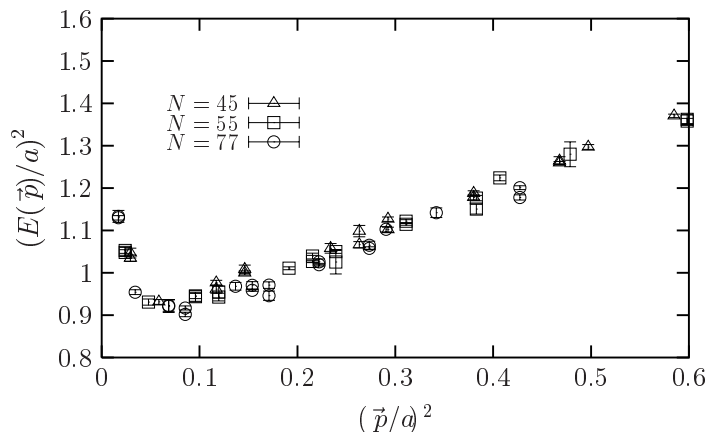


Figure 7. Dispersion relation in dimensional units, at $\lambda = 50$ and $N \Delta m^2 \simeq 100$. Both axes are given in units of M_{eff}^2 . We see that the dispersion stabilises, so it is possible to take a DSL next to the striped phase, with a finite width of the stripes to be formed at $m^2 < m_c^2$.

occur in the NC plane. However, the proof for this theorem is based on assumptions of standard quantum field theory, like locality — this does not hold on the NC plane.

Still, Gubser and Sondhi did not expect a striped phase in $d = 2$ [12]. They presented a consideration how the Mermin-Wagner Theorem could be extended even to NC field theory. They used an effective action approach of the Brazovskii-type, where the kinetic term is of quartic order in the momentum, which should make the exclusion of spontaneous symmetry breaking stronger. On the other hand, the effective action approach of Ref. [16] seems to affirm a striped phase.

From the numerical side, a striped phase in the NC $\lambda\phi^4$ model has been manifestly observed also in $d = 2$ [11, 17, 18]. However, this does not prove its existence in the DSL — it could also be an artifact of the lattice and of finite volume. The fate of this phase in the DSL has been investigated numerically only very recently [19].

The matrix model formulation corresponds to the description in Subsection 2.1, where the time direction collapses to one site. Figure 8 shows the phase diagram in $d = 2$. We see that the vertical axis needs a scaling factor $N^{3/2}$, which differs from the 3d case (cf. Figure 1). If m^2 is scaled in this way, we observe a convincing stabilisation of the order/disorder transition line for $N \geq 19$.

Figure 9 shows again typical configurations in the four sectors of this phase diagram, in analogy to the Figure 2, but now with a four-stripe pattern. The transition was again detected with the order parameter (2.6). Figure 10 gives examples how the uniform or striped order parameter rises for decreasing m^2 , and how the corresponding connected correlator exhibits a peak at the transition.

Now we consider also here the correlation function. In $d = 3$ we focused on the correlation in time direction in order to extract the dispersion relation and to introduce the effective mass M_{eff} , as a scale for the DSL. This is not available anymore in $d = 2$, so now we have to deal with the spatial correlation, and its unusual decay behaviour. Figure 11 shows an example in the disordered phase, but next to the the striped phase — for slightly lower m^2 a 4-stripe pattern will condense (like the example in Figure 9 on the bottom at the right).

Our concept is as follows: we decrease m^2 down towards m_c^2 , and we increase the matrix size N at the same time, such that the decay of the correlator stabilises down to the first dip. This replaces the usual reference to the exponential decay. The difference Δm^2 , defined in eq. (2.11),

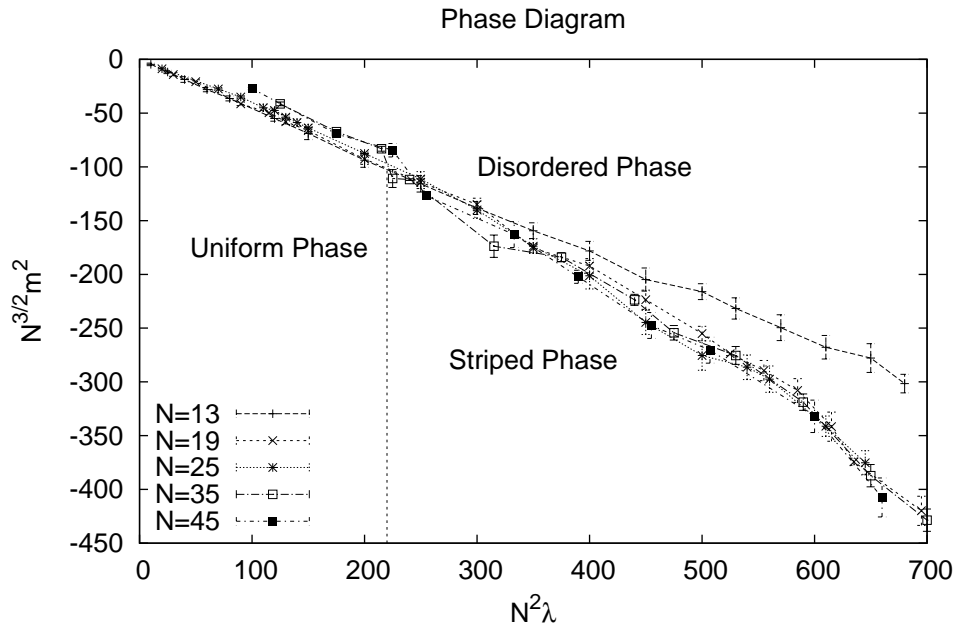


Figure 8. The phase diagram of the 2d NC $\lambda\phi^4$ model. In contrast to the 3d case, the vertical axis has to be chosen as $N^{3/2}m^2$. Then the transition line between disorder and the ordered phases stabilises at $N \geq 19$.

introduces a scale, which translates — with a suitable exponent — into the scale of the DSL,

$$a^2 \propto (\Delta m^2)^\sigma . \tag{3.1}$$

The exponent σ has to be identified, then we can address the question whether or not it is possible to take a DSL and keep close to the striped phase. If this can (cannot) be done, this is evidence for the existence (absence) of the striped phase in the continuum and infinite volume limit of this model.

To tackle this question, we first choose a normalisation by setting the lattice spacing for $N = 35$ to $a = 1$. Thus the DSL converts a lattice distance x into the dimensional distance

$$ax = \sqrt{\frac{35}{N}} x . \tag{3.2}$$

This distance should be compatible up to the first correlation dip for increasing N .

In analogy to the “dimensionless temperature”, which is often used near a phase transition, $(T - T_c)/T_c$, we adjust the dimension by the suitable power of m_c^2 , such that the DSL can be written as

$$Na^2 = N \frac{(\Delta m^2)^\sigma}{(m_c^2)^{1-\sigma}} . \tag{3.3}$$

Now let us consider two matrix sizes N_1 and N_2 ; we want to identify the mass shifts Δm_1^2 and Δm_2^2 which correspond to the same trajectory towards the DSL. We fix λ to the same value, so that the dimensionless term $\lambda\theta$ remains constant. We fine-tune the mass shifts such that they lead to the same short-distance correlation decay. This is illustrated for three examples in

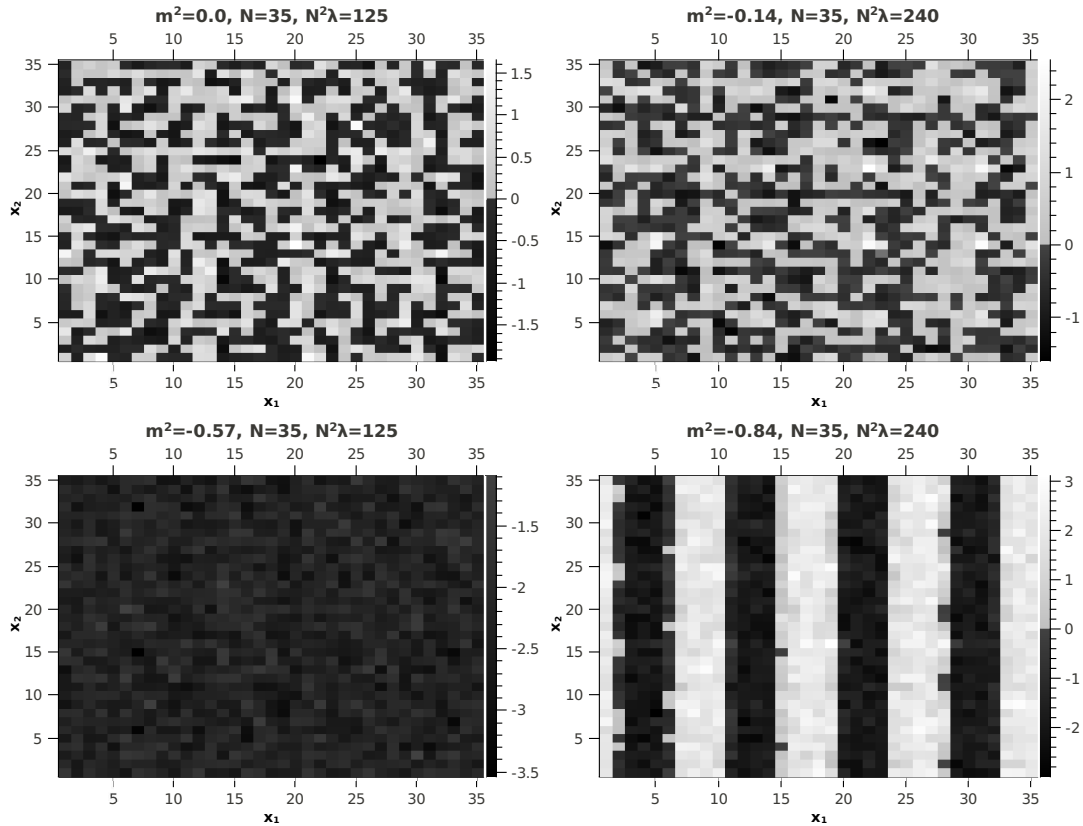


Figure 9. Typical configurations in four sectors of the phase diagram in Figure 8, analogous to Figure 2. The upper plots are in the disordered phase, next to the uniform and to the striped phase, respectively. The lower plots are examples for uniform and for striped ordering.

Figure 12. Once these values Δm_i^2 ($i = 1, 2$), and the corresponding critical values $m_{c,i}^2$, are determined, we extract the exponent σ from

$$\sigma = \frac{\ln(m_{1,c}^2/m_{2,c}^2)}{\ln(\Delta m_{1,c}^2/\Delta m_{2,c}^2) + \ln(m_{1,c}^2/m_{2,c}^2)}. \quad (3.4)$$

This has to be done for a variety of pairs N_1 , N_2 , and the crucial question is whether or not a stable σ -value is obtained.

λ	N_1	N_2	σ
0.222	35	45	0.152(7)
	35	55	0.156(6)
	45	55	0.161(11)
0.286	25	35	0.161(9)
	25	45	0.167(7)
	35	45	0.178(23)
0.4	25	35	0.147(13)

Table 1. The σ -values obtained for various pairs of sizes N_1 , N_2 after tuning Δm^2 such that the short-distance decay of the correlation function coincides.

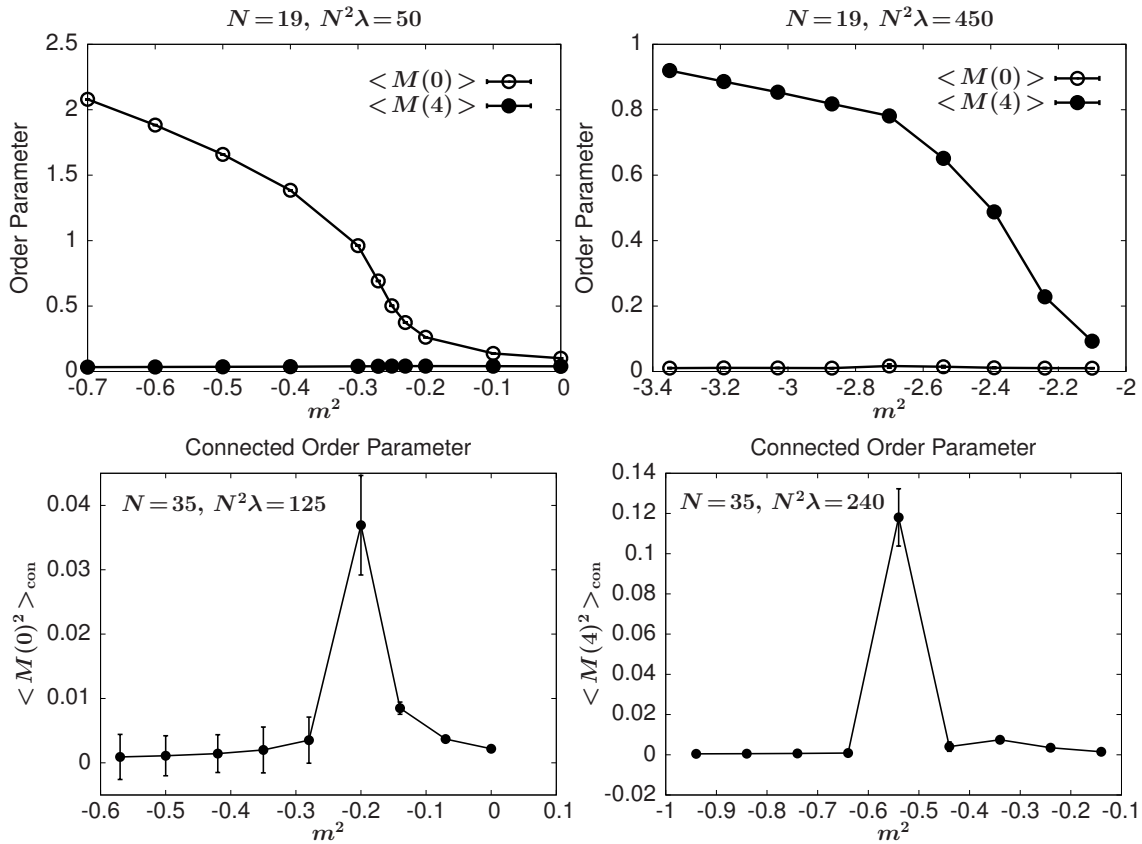


Figure 10. The order parameters $\langle M(0) \rangle$ and $\langle M(4) \rangle$, as defined in eq. (2.6), for the 2d NC $\lambda\phi^4$ model. We keep N and λ fixed and show the dependence on m^2 . Above we see that for small (large) λ and decreasing m^2 the disorder turns into a uniform (4-stripe) pattern. Below we show examples where the 2-point functions of these order parameters have a peak, which allows us to identify the critical value m_c^2 .

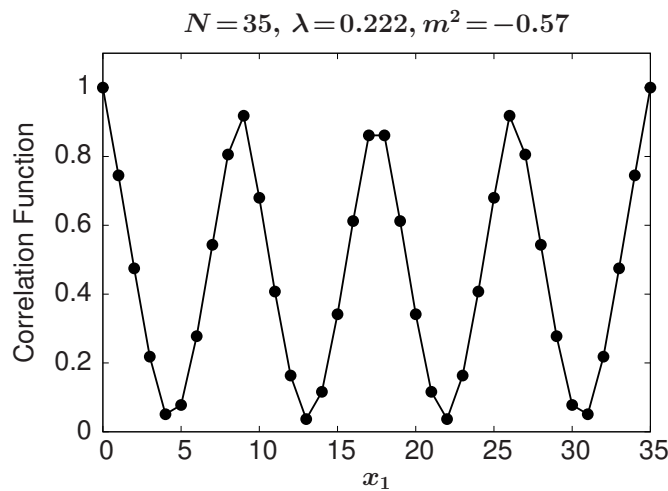


Figure 11. The correlation function $\langle \phi_{(0,0)} \phi_{(x_1,0)} \rangle$ near the striped phase, at $(N^{3/2}m^2, N^2\lambda) = (-118, 272)$. For somewhat lower m^2 a 4-stripe pattern condenses.

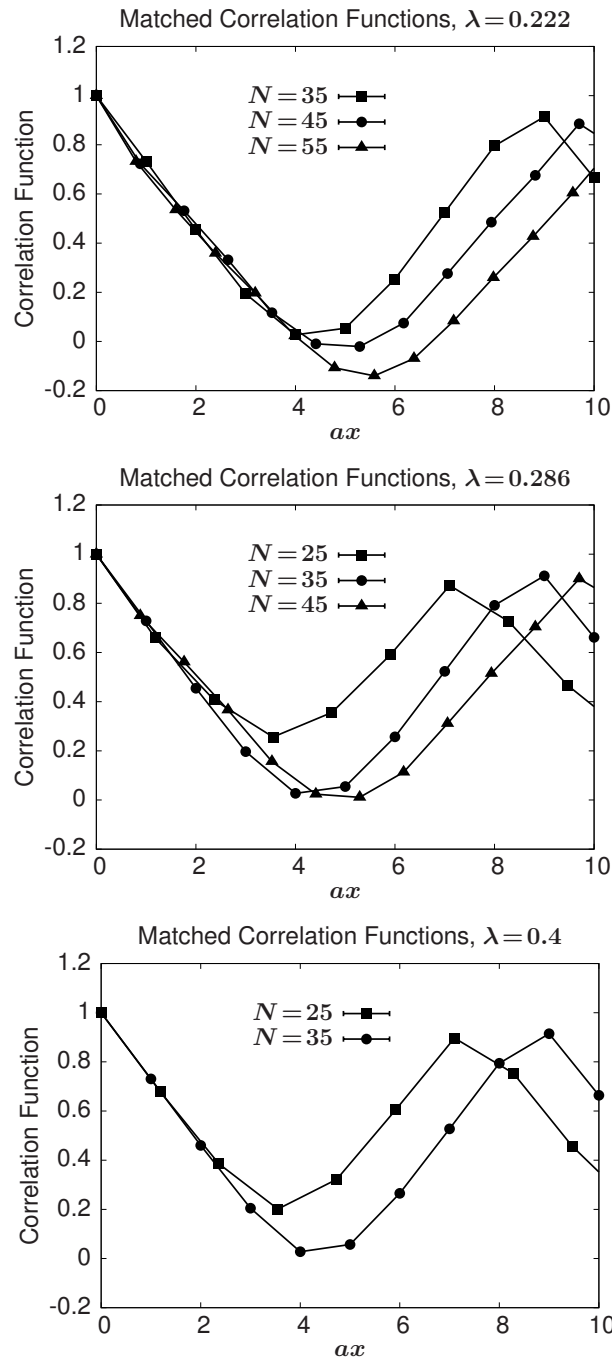


Figure 12. Three examples for “matched correlation functions”: at fixed λ , but for different sizes N , the parameter $\Delta m^2 = m^2 - m_c^2$ is tuned such that the correlation decay down to the first dip has the same slope. Then the distance in physical units — as given in eq. (3.2) — agrees. In this way we identify Δm^2 values to be inserted in eq. (3.4), which determines the exponent σ .

There are practical constraints for these evaluations: λ has to be large enough to be close to the striped (not uniform) phase for the smaller N involved. On the other hand, for the larger N the product $N^2\lambda$ should not be too large — otherwise we run to the far right in the

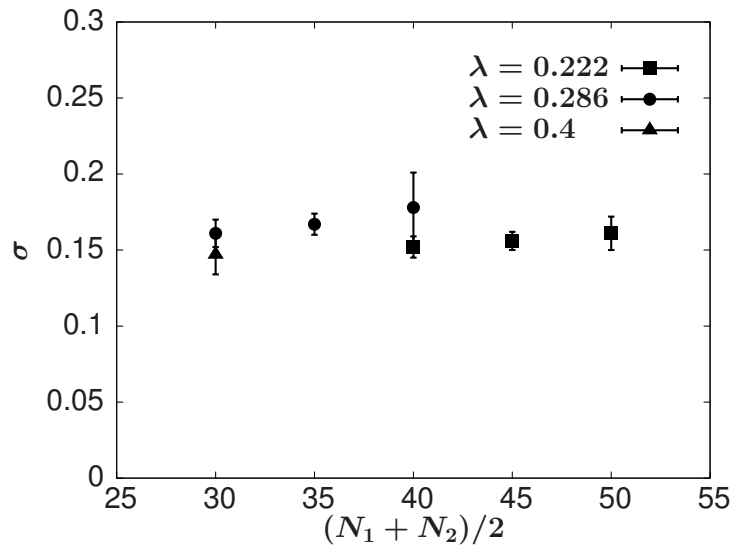


Figure 13. An illustration of the values given in Table 1. We see a clear trend to a plateau value of $\sigma = 0.16(1)$.

phase diagram in Figure 8, where the effective potential forms a landscape of many deep valleys (meta-stable local minima), so reliable simulations are more and more difficult to achieve (the trouble starts already with the thermalisation).

Still a numerically accessible window could be found, and we give our results for three λ values in Table 1 and Figure 13. We considered the uncertainties which affect σ (errors in Δm_i^2 and in $m_{c,i}^2$), but the precision is sufficient to confirm a clear trend towards a stable exponent

$$\sigma = 0.16(1) . \quad (3.5)$$

Thus we can indeed approach the DSL consistently, running to the right in the phase diagram in Figure 8, while staying in the vicinity of the striped phase. This implies that the latter does persist in the DSL. Hence in the NC world translation symmetry can indeed break spontaneously, even in $d = 2$.

4. Conclusions

We have studied the $\lambda\phi^4$ model in $d = 3$ [11] and in $d = 2$ [19]. In both cases, the spaces include a non-commutative plane. In order to explore this model beyond perturbation theory, we introduced a (fuzzy) lattice regularisation and mapped the theory onto a Hermitian matrix model, following Ref. [10]. This enables Monte Carlo simulations, which were performed with a Metropolis algorithm.²

For both dimensions we observed that a strongly negative bare mass parameter m^2 enforces some order.

- If λ is small, so that non-commutativity effects are weak, this order is the uniform magnetisation, as in the commutative variant of this model.
- If λ is large, so that non-commutativity effects are strongly amplified, this order is “striped”. That phase does not occur in the commutative case.

² There have been related studies of the $\lambda\phi^4$ model on a *fuzzy sphere* instead of a NC plane [20]. Also in that case Monte Carlo simulations were performed after the mapping onto a Hermitian matrix model. However, the non-commutativity relation differs from the form (1.1) that we have discussed here.

In both dimensions we gave numerical evidence that the striped phase persists in the Double Scaling Limit, which extrapolates simultaneously to the continuum and to infinite volume, while keeping the non-commutativity parameter θ fixed. This indicates the spontaneous breaking of translation and rotation symmetry in this limit.

For the 2d case this might appear surprising due to the Mermin-Wagner Theorem. However, this theorem does not apply to non-commutative field theory, since it assumes locality and an IR regular behaviour.

Acknowledgments

Part of the results presented here are based on our collaboration with Jun Nishimura. We thank him, as well as Antonio Bigarini and Jan Volkholz, for their contributions, and Urs Gerber for reading the manuscript.

This work was supported by the Mexican *Consejo Nacional de Ciencia y Tecnología* (CONA-CyT) through project 155905/10 “Física de Partículas por medio de Simulaciones Numéricas”, and by the Spanish *MINECO* (grant SEV-2012-0249). The recent simulations were performed on the cluster of the Instituto de Ciencias Nucleares, UNAM.

- [1] Snyder H S 1947 *Phys. Rev.* **71** 38
Yang C-N 1947 *Phys. Rev.* **72** 874
- [2] Connes A 1995 *J. Math. Phys.* **36** 6194
- [3] Girvin S M 1999 arXiv:cond-mat/9907002 [cond-mat.mes-hall]
- [4] <http://inspirehep.net/>
- [5] Seiberg N and Witten E 1999 *JHEP* **09** 032
- [6] Doplicher S, Fredenhagen K and Roberts J E 1995 *Commun. Math. Phys.* **172** 187
- [7] Filk T 1996 *Phys. Lett. B* **376** 53
- [8] Szabo R J 2003 *Phys. Rept.* **378** 207
- [9] Minwalla S, Van Raamsdonk M and Seiberg N 2000 *JHEP* **0002** 020
- [10] Ambjørn J, Makeenko Y M, Nishimura J and Szabo R J 2000 *JHEP* **05** 023
- [11] Bietenholz W, Hofheinz F and Nishimura J 2003 *Acta Phys. Polonica B* **34** 4711; 2004 *JHEP* **0406** 042
Hofheinz F 2004 *Fortsch. Phys.* **52** 391
- [12] Gubser S S and Sondhi S L 2001 *Nucl. Phys. B* **605** 395
- [13] Chen G-H and Wu Y-S 2002 *Nucl. Phys. B* **622** 189
- [14] Castorina P and Zappalà D 2002 *Phys. Rev. D* **68** 065008
Mandanici G 2004 *Int. J. Mod. Phys. A* **19** 3541
Hernández J M, Ramírez C and Sánchez M 2013 *Phys. Rev. D* **87** 125012
- [15] Mermin D and Wagner H 1966 *Phys. Rev. Lett.* **17** 113
- [16] Castorina P and Zappalà D 2008 *Phys. Rev. D* **77** 027703
- [17] Bietenholz W, Hofheinz F and Nishimura J 2003 *Nucl. Phys. (Proc. Suppl.)* **119** 941
- [18] Ambjørn J and Catterall S 2002 *Phys. Lett. B* **549** 253
- [19] Mejía-Díaz H 2013 *Diagrama de fase del modelo $\lambda\phi^4$ bidimensional no-conmutativo*
B.Sc. thesis, Universidad Nacional Autónoma de México
Mejía-Díaz H, Bietenholz W and Panero M, in preparation
- [20] Martin X 2004 *JHEP* **0404** 077
Panero M 2006 *SIGMA* **2** 081; 2007 *JHEP* **0705** 082
Medina J, Bietenholz W and O’Connor D 2008 *JHEP* 0804 (2008) 041
García Flores F, Martin X and O’Connor D 2009 *Int. J. Mod. Phys. A* **24** 3917
Ydri B 2014 arXiv:1401.1529 [hep-th]